

## A Thermally Activated Exciton–Exciton Collision Process in ZnO Microrods

This article has been downloaded from IOPscience. Please scroll down to see the full text article.

2004 Chinese Phys. Lett. 21 1640

(<http://iopscience.iop.org/0256-307X/21/8/063>)

View [the table of contents for this issue](#), or go to the [journal homepage](#) for more

Download details:

IP Address: 221.8.12.150

The article was downloaded on 05/09/2012 at 06:19

Please note that [terms and conditions apply](#).

# A Thermally Activated Exciton–Exciton Collision Process in ZnO Microrods \*

ZHAO Dong-Xu(赵东旭)<sup>1</sup>, LIU Yi-Chun(刘益春)<sup>1,2\*\*</sup>, SHEN De-Zhen(申德振)<sup>1</sup>,  
LU You-Ming(吕有明)<sup>1</sup>, ZHANG Ji-Ying(张吉英)<sup>1</sup>, FAN Xi-Wu(范希武)<sup>1</sup>

<sup>1</sup>The Key Laboratory of Excited State Processes, Changchun Institute of Optics, Fine Mechanics and Physics,  
Chinese Academy of Sciences, Changchun 130022

<sup>2</sup>Centre for Advanced Optoelectronic Functional Material Research, Northeast Normal University, Changchun 130024

(Received 29 January 2004)

*Room-temperature P-band emission induced by an exciton–exciton collision process was observed in ZnO micro-rods. Both temperature- and excitation-intensity-dependent photoluminescence (PL) measurements were conducted. The excitation-intensity-dependent measurement illustrated that the P-band emission could occur at far lower excitation intensity than that reported in the literature. Higher-order transitions were also observed at the excitation intensity of 7.1 kW/cm<sup>2</sup> or above. The temperature-dependent PL showed that the P-band emission process was thermally activated. It is suggested that both the density and activity of free excitons played important roles in the exciton–exciton collision process.*

PACS: 78.55.Et, 78.67.Lt, 78.55.Hx, 81.05.Ea

ZnO is one of the wide-band gap semiconductors, which has a band-gap of 3.37 eV at room temperature and the exciton binding energy of 60 meV.<sup>[1–4]</sup> The high exciton binding energy ensures that excitonic survival is well above room temperature. Since the ultraviolet lasing of ZnO films was reported at room temperature in 1997, the study of the photoluminescence property of ZnO has attracted considerable interest.<sup>[5–7]</sup> This is largely due to the potential commercial value of ZnO for short-wavelength semiconductor diode lasers.<sup>[8–15]</sup> The mechanism of laser emission of ZnO thin films is believed to be exciton–exciton scattering at intermediate intensity excitation, however it may switch to electron–hole plasma emission at high intensity excitation.<sup>[9]</sup>

It is clear that a detailed understanding of the exciton–exciton collision process is very important for lowering the lasing threshold of ZnO. The theory of the exciton–exciton collision process was extensively studied in the 1970s.<sup>[16–19]</sup> The exciton–exciton collision process has been observed in bulk ZnO at cryogenic temperature<sup>[16–19]</sup> and in self-assembled ZnO microcrystallite thin films at room temperature.<sup>[9]</sup> It was also reported that the lasing threshold of a ZnO single crystal platelet was at 60 K rather than at 10 K when the sample was under-pulsed electron beam excitation.<sup>[20]</sup> However, there has been little discussion in the literature since then.

In this Letter, we report both on excitation-intensity- and temperature-dependent photoluminescence investigation of ZnO micro-rods. A thermally activated process was observed in the exciton–exciton collision process.

ZnO micro-rods were successfully fabricated by a simple thermal oxidation technique as reported elsewhere.<sup>[21]</sup> The size of micro-rods was  $\sim 10\ \mu\text{m}$  in diameter and  $\sim 3\ \text{mm}$  in length. The x-ray diffraction (XRD) measurement showed that these micro-rods were highly crystalline with a wurtzite structure.

In the photoluminescence (PL) experiment, the excitation source was a He–Cd cw laser at a wavelength of 325 nm. A UV JY63 micro-Raman spectrometer made in France was used to obtain PL spectra. An excitation laser beam was focused onto the sample by an objective lens ( $\times 10\ \text{UV}$ ) with a spot size of  $\sim 15\ \mu\text{m}$ . A charge-coupled-device (CCD) camera with a choice of high resolution ( $< 1\ \text{cm}^{-1}$ ) or wide spectral range was used to detect the emission spectra. A liquid nitrogen cooled temperature variable stage was used to carry out the temperature-dependent measurements. The thermal stability at any chosen temperature was  $< 1\ \text{K}$ .

Figure 1 shows the PL spectra of the ZnO micro-rods as a function of the excitation intensities at room temperature. The excitation intensity is changed from 700 W/cm<sup>2</sup> to 28.3 kW/cm<sup>2</sup>. At low excitation intensity there is only one PL band observed due to the free exciton emission (denoted by  $E_{ex}$ ) in the spectra. When the excitation intensity is increased to 2.1 kW/cm<sup>2</sup>, an additional emission band (denoted by  $P$ ) appears as a shoulder of the  $E_{ex}$  band with the photon energy of 75 meV below the  $E_{ex}$  band (from other reports the  $P$  band could be seen clearly under the excitation intensity of 7.5 kW/cm<sup>2</sup> or higher).<sup>[8,9]</sup> With the further increase of the excitation intensity, the intensity of the  $P$  band grows superlinearly. When the

\* Supported by the Hundred Talents Programme of Chinese Academy of Sciences, the Knowledge Innovation Project of Chinese Academy of Sciences, and the National Natural Science Foundation of China under Grant No 60176003.

\*\* To whom correspondence should be addressed. Email: ycliu@nenu.edu.cn

©2004 Chinese Physical Society and IOP Publishing Ltd

excitation intensity exceeds  $16 \text{ kW/cm}^2$ , the intensity of the  $P$  band dominates the PL spectra.

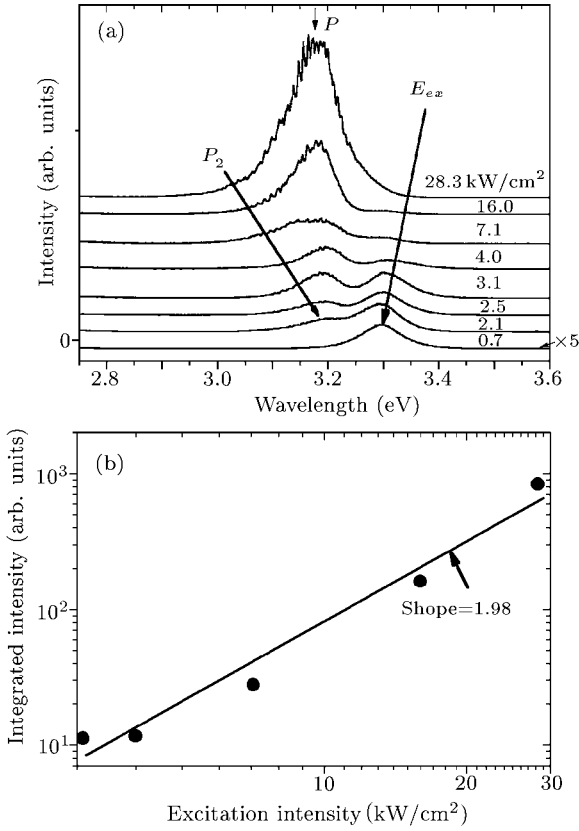


**Fig. 1.** (a) PL spectra of ZnO micro-rods under different excitation intensities at room temperature. (b) The integrated intensity of the  $P$  band as a function of the excitation intensity.

It is known that the  $P$  band is attributed to the radiative recombination of an exciton-exciton collision process. In the process, one of the two excitons takes energy from the other and scatters into a higher exciton state with a quantum number  $n > 1$ , while the other recombines radiatively.<sup>[16–19]</sup> The photons emitted in this process have the energies of  $E_n$  given by

$$E_n = E_{ex} - E_b^{ex} \left(1 - \frac{1}{n^2}\right) - \frac{3}{2}kT, \quad n = 2, 3, 4, \dots, \infty \quad (1)$$

where  $E_{ex}$  is the free-exciton emission energy,  $E_b^{ex} = 60 \text{ meV}$  is the binding energy of the free exciton,  $n$  is the quantum number of the envelope function, and  $kT$  is the thermal energy.<sup>[9,19]</sup> At room temperature, according to Eq. (1), the values of  $E_{ex} - E_n$  are 83, 91, and 98 meV for  $n = 2, 3$ , and 8, respectively, which are in good agreement with the experimental results. The quantitative analysis shows a quadratic relation between the  $P$  intensity and excitation intensity when the intensity changes in the range 2.1–4.0  $\text{kW/cm}^2$ . A linear fit led to a slope of 1.98. Thus, it is confirmed that this band is  $P_2$  emission. At 7.1  $\text{kW/cm}^2$ , an ad-

ditional  $P$  band can be clearly seen as a shoulder at lower photon energy side.

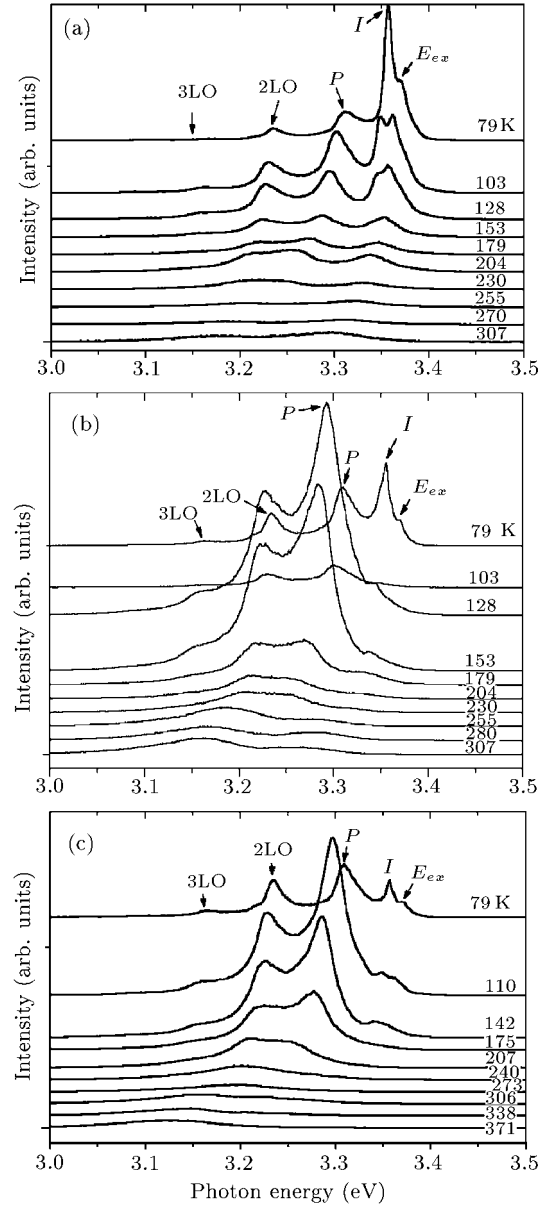


**Fig. 2.** PL spectra of ZnO micro-rods over a wide temperature range under different excitation intensities: (a) 2.1  $\text{kW/cm}^2$ , (b) 2.5  $\text{kW/cm}^2$ , (c) 4.0  $\text{kW/cm}^2$ .

Figure 2 shows the temperature-dependent emission spectra of ZnO micro-rods from 79 K to 458 K with the excitation intensity of 2.1, 2.5 and 4.0  $\text{kW/cm}^2$ , respectively. Unlike reports in the literature, there were five peaks observed at 79 K. These peaks are denoted as  $E_{ex}$ ,  $I$ ,  $P$ , 2LO and 3LO, respectively. The  $E_{ex}$  and  $I$  emission bands are due to free exciton emission and excitons bound to neutral donor or acceptor transitions. The 2LO and 3LO emission peaks located at  $\sim 135 \text{ meV}$  and  $205 \text{ meV}$  below the  $E_{ex}$  band are from the phonon replicas of

the free exciton. The  $P$  band is attributed to the emission from the exciton–exciton collision process as discussed earlier. The photon energy is  $\sim 58$  meV below the  $E_{ex}$  band, which agrees well with the calculated value from Eq. (1). Because the  $P$  band emission at low temperature is strong and very close to the 1LO band, which is enveloped by the  $P$ -band, the 1LO band could not be seen clearly in the spectra. For the sample excited below  $2.1 \text{ kW/cm}^2$ , the luminescence spectra are dominated by the bound exciton emission at low temperature. With the increase of the temperature the intensity of  $I$  band decreases sharply. When the temperature is increased above 128 K, the emissions from  $E_{ex}$  and  $P$  bands dominate the emission spectra. When the excitation intensity reaches to  $2.5 \text{ kW/cm}^2$  and  $4.0 \text{ kW/cm}^2$ , the  $P$  band gradually dominates in the spectra with the increase of the temperature.

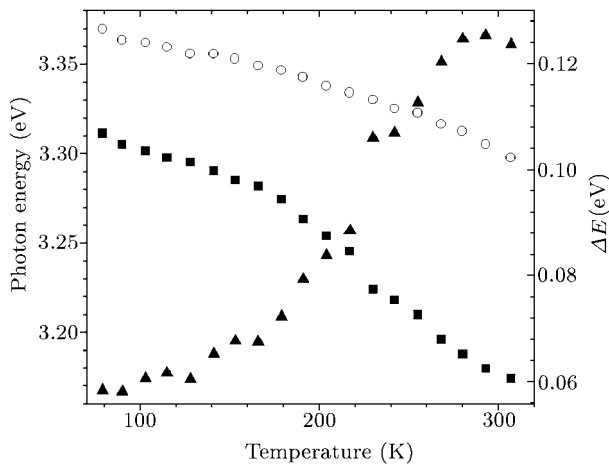


**Fig. 3.** Peak positions of  $E_{ex}$  (open dots) and  $P$  (solid squares) bands versus temperature (triangles:  $\Delta E = E_{ex} - P$ ).

Figure 3 illustrates the peak positions of  $E_{ex}$  (open dots) and  $P$  bands (solid squares) together with the energy separation (up-triangles) between  $E_{ex}$  and  $P$  bands as a function of temperature. The excitation intensity is  $2.1 \text{ kW/cm}^2$  as shown in Fig. 2(a). As the temperature increases, the emission photon energies of  $E_{ex}$  and  $P$  bands shift to the low energy gradually. Their energy difference increases linearly first and then reaches saturation at  $T > 255 \text{ K}$ . The values of  $\Delta E$  ( $E_{ex} - P_2$ ) calculated from Eq. (1) agree well with the experimental data with temperature suggesting that one of the two excitons is scattered into the excitation state of  $n = 2$  during the collision process. At  $T > 180 \text{ K}$ , the value of  $\Delta E$  grows quickly with the temperature. It is argued that the drastic increase of the  $P$ -band is due to the additional transitions from the higher order scattering for  $n > 2$  at higher temperature. The higher excitation energies at  $2.5 \text{ kW/cm}^2$  and  $4.0 \text{ kW/cm}^2$  shows similar features as illustrated

in Fig. 3.

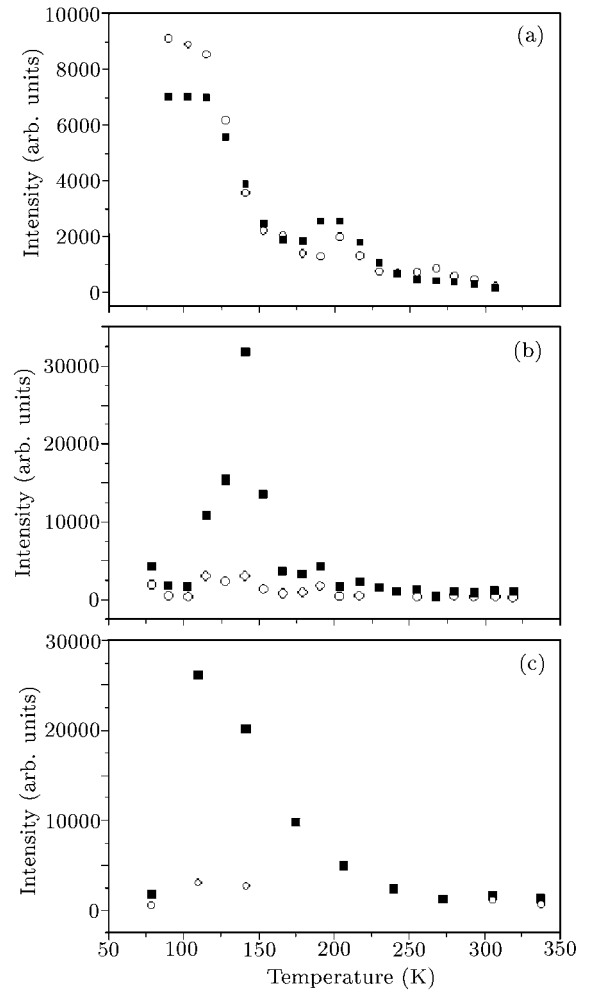


**Fig. 4.** Intensities of  $E_{ex}$  (open dots) and  $P$  (solid squares) bands versus temperature: (a)  $2.1 \text{ kW/cm}^2$ , (b)  $2.5 \text{ kW/cm}^2$ , (c)  $4.0 \text{ kW/cm}^2$ .

The emission intensities of  $E_{ex}$  (open circles) and  $P$  (solid squares) bands as a function of temperature are illustrated in Fig. 4. When the excitation intensity is at  $2.1 \text{ kW/cm}^2$ , the PL intensities of  $E_{ex}$  and  $P$  bands decrease gradually with the increasing temperature in the low temperature region. The intensity of  $E_{ex}$  band is higher than that of the  $P$  band. When the temperature is raised to 150 K, the intensity of  $P$  band becomes stronger than that of the  $E_{ex}$  band and reaches a maximum value at 200 K. The intensity of free exciton emission also shows a peak value at the same temperature. Then, both intensities of  $E_{ex}$  and  $P$  bands decrease again with the further increase of temperature. When the excitation intensity increases to  $2.5 \text{ kW/cm}^2$  and  $4.0 \text{ kW/cm}^2$ , the  $P$  band emission intensity becomes stronger than that of the  $E_{ex}$  band in the entire temperature range as shown in Figs. 4(b) and 4(c). The maximum value of the  $P$  emission intensity is clearly shifted to lower temperature as the excitation intensity is increased. Because the exciton

density increases with increasing excitation intensity, the probability of the exciton–exciton scattering also increases, which induces that the maximum in intensity of the *P* band shift to lower temperature.

Based on the above experimental results, a thermally activated process for the exciton–exciton collision is suggested. In order to explain the *P* emission intensity peak shift with temperature both density and activity of the photogenerated free excitons are considered. When the sample is illuminated with fixed excitation intensity, the density of the photogenerated free excitons is high at low temperature. The free excitons at low temperature are localized, which leads to low probability of exciton–exciton collision. Thus, the *P* emission band is peaked in a low temperature range. With the increase of the temperature, although the density of the free excitons decreases, the excitonic activity is increased. Hence, the collision rate between exciton–exciton is also increased drastically. Further increase of temperature leads to the appearance of the excitonic ionization process as the result of thermal activation. Thus, the interplay of both the effects presented above leads to the observed *P*-band emission maximum at particular temperature for a fixed excitation intensity.

In conclusion, we have conducted both temperature- and excitation-intensity-dependent PL measurements. The temperature-dependent PL shows an existence of the *P*-band intensity maximum emission at a particular temperature. This maximum emission is also dependent on the excitation intensity. A thermally activated process is proposed. In this process, both the density and the activity of free

excitons play important roles.

## References

- [1] Hvam J M 1971 *Phys. Rev. B* **4** 4459
- [2] Huang H and Kock S 1975 *Phys. Status Solidi B* **82** 531
- [3] Klingshirn C 1994 *Adv. Mater. Opt. Electron.* **3** 103
- [4] Klingshirn C 1975 *Phys. Status Solidi B* **71** 547
- [5] Guo B, Ye H and Qiu Z R 2003 *Chin. Phys. Lett.* **20** 1571
- [6] Xu C X, Sun X W, Chen B J, Sun C Q, Tay B K, Li S X and Sean 2003 *Chin. Phys. Lett.* **20** 1319
- [7] Xiang W H, Zhang G Z, Sun Y, Wang G and Ketterson J B 2003 *Chin. Phys. Lett.* **20** 296
- [8] Bagall D M, Chen Y F, Zhu Z, Yao T, Koyama S, Shen M Y and Goto T 1997 *Appl. Phys. Lett.* **70** 2230
- [9] Tang Z K, Yu P, Wong G K L, Kawasaki M, Ohotomo A, Koinuma H and Segawa Y 1997 *Solid State Commun.* **103** 459
- [10] Tang Z K, Yu P, Wong G K L, Kawasaki M, Ohotomo A, Koinuma H and Segawa Y 1997 *Nonlinear Opt.* **18** 355
- [11] Tang Z K, Wong G K L, Yu P, Kawasaki M, Ohotomo A, Koinuma H and Segawa Y 1998 *Appl. Phys. Lett.* **72** 3270
- [12] Bagnall D M, Chen Y F, Shen M Y, Zhu Z, Goto T and Yao T 1998 *J. Cryst. Growth* **184/185** 605
- [13] Sun H D, Makino T, Tuan N T, Segawa Y, Tang Z K, Wong G K L, Kawasaki M, Ohtomo A, Tamura K and Koinuma H 2000 *Appl. Phys. Lett.* **77** 4250
- [14] Sun H D, Makino T, Segawa Y, Kawasaki M, Ohtomo A, Tamura K and Koinuma H 2002 *J. Appl. Phys.* **91** 1993
- [15] Ohashi N, Sekiguchi T, Aoyama K, Ohgaki T, Terada Y, Sakaguchi I, Tsurumi T and Haneda H 2002 *J. Appl. Phys.* **91** 3658
- [16] Magde D and Mahr H 1970 *Phys. Rev. Lett.* **24** 890
- [17] Hvam J M 1974 *Phys. Status Solidi B* **63** 511
- [18] Klingshirn C 1975 *Phys. Status Solidi B* **71** 547
- [19] Koch S W, Haug H, Schmieder G, Bohnert W and Kingshirn C 1978 *Phys. Status Solidi B* **89** 431
- [20] Hvam J M 1973 *Solid State Commun.* **12** 95
- [21] Zhao D X, Liu Y C, Shen D Z, Lu Y M, Zhang J Y and Fan X W 2003 *J. Appl. Phys.* **94** 5605